4-20-2009

The rotational spectrum of the FeD radical in its X4Δ state, measured by far-infrared laser magnetic resonance

Michael Jackson

Lyndon R. Zink

Jonathan P. Towle

Neil Riley

John M. Brown

The rotational spectrum of the FeD radical in its $X\ ^4\Delta$ state, measured by far-infrared laser magnetic resonance

Michael Jackson,[1] Lyndon R. Zink,[2] Jonathan P. Towle,[3] Neil Riley,[3] and John M. Brown[3,a)]
[1]*Department of Physics, Central Washington University, Ellensburg, Washington 98926-7422, USA*
[2]*Department of Physics, University of Wisconsin-La Crosse, La Crosse, Wisconsin 54601, USA*
[3]*Department of Chemistry, The Physical and Theoretical Chemistry Laboratory, Oxford University, South Parks Road, Oxford OX1 3QZ, United Kingdom*

(Received 23 January 2009; accepted 2 March 2009; published online 20 April 2009)

Transitions between the spin-rotational levels of the FeD radical in the $v=0$ level of the $X\ ^4\Delta$ ground state have been detected by the technique of laser magnetic resonance at far-infrared wavelengths. Pure-rotational transitions have been observed for the three lowest spin components. Lambda-type doubling is resolved on all the observed transitions; nuclear hyperfine structure is not observed. The energy levels of FeD are strongly affected by the breakdown of the Born–Oppenheimer approximation and cannot be modeled accurately by an effective Hamiltonian. The data are therefore fitted to an empirical formula to yield term values and g-factors for the various spin-rotational levels involved. © *2009 American Institute of Physics*. [DOI: 10.1063/1.3117182]

I. INTRODUCTION

The FeH radical has been intensively studied over the past 40 years following its identification through the observation of its electronic spectrum.[1,2] There are two reasons for this continuing interest. First, there is the role that it plays in astronomy. FeH was identified as a significant component of the atmospheres of the sun and other "cool" stars of spectral types M, S, and K some time ago.[2,3] More recently, it has emerged as an important probe of the physical conditions of even cooler stars and substellar objects.[4–6] Such applications require a detailed knowledge on the molecule's spectroscopic and magnetic properties. The second motivation for the study of FeH is a desire to understand its electronic structure. This turns out to be the most complicated of all the first-row transition metal hydrides, as evidenced by both theoretical[7] and experimental works.[8–10] Indeed, despite a large number of separate spectroscopic studies,[11–26] the surface of this problem has barely been scratched. There is a simple reason for the complexity of the electronic structure of FeH. The easy rearrangement of the electrons within the open d-shell orbitals results in a large number of electronic states of similar energies. In the case of FeH, the separation between electronic states is smaller than that between its vibrational levels.[7,14] As a result, there is a catastrophic breakdown of the Born–Oppenheimer separation for this molecule. The various electronic states perturb each other strongly (through spin-orbit and rotational mixings) and the individual rotational levels cannot even be modeled by the standard effective Hamiltonian.[27] A long-term objective of the current studies of the electronic spectrum of FeH is to gather information on as many states as possible so that they can be fitted all together, along the lines of that achieved for NiH (the super-multiplet model[28,29]). Another source of information on the perturbations between the electronic states of FeH is the study of its isotopologue FeD. The vibrational and rotational energies of a diatomic molecule depend on its reduced mass but the electronic energy, to a good approximation, does not; the interstate mixings therefore occur at different v and J values in FeD and so throw a different light on their nature. The present paper, concerned with the rotational spectrum of FeD, is thus a contribution to the study of the electronic structure of FeH.

In fact, there have been very few previous studies of FeD. A major contribution was made in 1983 by Balfour *et al.*[30] who succeeded in performing a rotational analysis of two vibrational bands in the $F\ ^4\Delta$-$X\ ^4\Delta$ transition of FeD in the near infrared. This paper provided information on the rotational and vibrational energy levels and on the nature of the two electronic states involved. About the same time, Stevens *et al.*[12] recorded the laser photoelectron spectrum of FeH^- and FeD^-. A careful analysis of their results strongly suggested that the electronic ground state of FeH is $^4\Delta$ with a $^6\Delta$ state only 1945 cm^{-1} above it; these proposals have been confirmed subsequently. Their study also provided the first reliable measurements of the vibrational wavenumbers of FeH and FeD in the ground electronic state.

In the present paper, we report much more accurate measurements of the rotational spectrum of FeD in the $v=0$ level of its $X\ ^4\Delta$ state. The spectrum is recorded by the technique of laser magnetic resonance (LMR) at far-infrared wavelengths, appropriate to the fairly large rotational constant of this molecule (3.436 cm^{-1}). The spectrum is recorded by tuning individual M-components of the rotational transition into resonance with a fixed-frequency far-infrared laser by application of a variable magnetic field. As a consequence, information is obtained on the magnetic properties of FeD at the same time. The observations are fitted with an empirical model that provides values for the rotational intervals and the magnetic properties separately.

a)Author to whom correspondence should be addressed. Tel.: (44)-1865-275403. FAX: (44)-1865-275410. Electronic mail: jmb@physchem.ox.ac.uk.

TABLE I. Summary of observations in the far-infrared LMR spectrum of FeD in its $X\,^4\Delta$ state.

FeD transitions observed			Laser line			
Ω	J	Parity	λ (μm)	ν (GHz)	Gas	Pump
Rotational transitions						
7/2	$4\frac{1}{2}$-$3\frac{1}{2}$	$\mp \leftarrow \pm$	373.6	802.4928	N_2H_4	10R(12)
			369.1	812.1954	CH_3OH	9P(16)
	$5\frac{1}{2}$-$4\frac{1}{2}$	$\pm \leftarrow \mp$	305.7	980.5916	CH_3OD	9R(8)
			302.0	992.7089	CH_3OH	9P(14)
	$6\frac{1}{2}$-$5\frac{1}{2}$	$\mp \leftarrow \pm$	256.0	1170.9410	CH_2F_2	9P(24)
			253.7	1181.5889	CD_3OH	10R(36)
5/2	$3\frac{1}{2}$-$2\frac{1}{2}$	$\pm \leftarrow \mp$	418.7	715.9876	CD_3OH	10R(36)
			416.5	719.7511	CH_3OH	9P(14)
	$4\frac{1}{2}$-$3\frac{1}{2}$	$\mp \leftarrow \pm$	328.6	912.3739	$^{13}CH_3OH$	9P(12)
			326.4	918.4170	CH_2F_2	9R(14)
	$5\frac{1}{2}$-$4\frac{1}{2}$	$\pm \leftarrow \mp$	268.6	1116.2450	$^{13}CH_3OH$	10R(16)
			267.4	1120.9577	CH_3OH	10R(34)
3/2	$2\frac{1}{2}$-$1\frac{1}{2}$	$\mp \leftarrow \pm$	556.9	538.3473	CD_3I	10P(36)
			554.4	540.7831	CH_2CF_2	10P(14)
	$3\frac{1}{2}$-$2\frac{1}{2}$	$+\leftarrow -$	392.1	764.6426	CH_3OH	9P(36)
1/2	$2\frac{1}{2}$-$1\frac{1}{2}$	$-\leftarrow +$	513.0	584.3882	HCOOH	9R(28)

II. EXPERIMENTAL DETAILS

The far-infrared LMR spectra were recorded in the Physics Department at the University of Wisconsin-La Crosse using the spectrometer constructed originally by Evenson at the Boulder laboratories of NIST; the spectrometer has been described in detail elsewhere.[31] The FeD radicals were produced in the spectrometer sample volume by the reaction of deuterium atoms with $Fe(CO)_5$ vapor in a flow system, the D atoms being generated by passing a mixture of D_2 in helium through a microwave discharge operating at 2450 MHz. The total pressure in the sample volume was 1.5 Torr (200 Pa); the partial pressure of D_2 was 50 mTorr (6.6 Pa) and that of $Fe(CO)_5$ was 7 mTorr (0.9 Pa). Under these conditions, a black deposit of finely divided iron powder was put down in the reaction zone and the reaction cell needed frequent cleaning. The magnetic field was modulated at a frequency of 5.2 kHz and the signal detected with a lock-in amplifier at the same frequency. The resonances were consequently displayed as the first derivative of an absorption profile. The magnetic flux densities were measured at the start and end of each scan, typically over 10 mT, using the probe of a proton NMR gaussmeter mounted on one of the magnet pole pieces; the measurement of each resonance was then made by linear interpolation. The resultant experimental uncertainties were between 0.13 and 0.3 mT, depending on the signal-to-noise ratio. The errors of measurement of each resonance included in the least-squares fit depended on four factors, the uncertainty in measurement of the flux densities (discussed above), the accuracy of the laser frequency (which varied from 2 to 5 parts in 10^7), the setting of the laser to the top of its gain curve, and the signal-to-noise ratio. It is quite a complicated exercise to estimate the uncertainty in each individual resonance. Consequently, we have assigned the same uncertainty of 2 MHz to each resonance; this is a figure based on experience of making such measurements in a range of far-infrared LMR spectra.[32–34]

III. RESULTS AND ANALYSIS

A. Experimental observations

The four spin components of the $X\,^4\Delta$ state of FeD lie in an inverted order, with $\Omega=7/2$ lowest and $\Omega=1/2$ highest in energy. The separation between successive spin components is approximately 200 cm^{-1}.[10] Rotational transitions of FeD in the lowest three spin components of the $v=0$ level of the $X\,^4\Delta$ state have been detected by the technique of far-infared LMR spectroscopy; a tentative detection of a transition in the highest $^4\Delta_{1/2}$ component is also reported. A summary of the various rotational transitions detected is given in Table I, together with the details of the laser lines employed. The transitions are also shown on the energy level diagram in Fig. 1.

An example of the observed LMR spectra of FeD is given in Fig. 2. It shows the survey spectrum for the 369.1 μm laser line in π polarization (that is, with the oscillating electric field parallel to the applied magnetic field B_Z inducing $\Delta M_J=0$ transitions). The rotational transition involved is $J=4\frac{1}{2}\leftarrow 3\frac{1}{2}$ in the lowest $\Omega=7/2$ spin component. On closer inspection, each experimental signal consists of a closely spaced doublet, arising from lambda-type doubling. Another example, shown in closeup, is given in Fig. 3. In this case, the spectrum is recorded with the 302.0 μm laser line in σ polarization ($\Delta M_J=\pm 1$ transitions); the rotational transition involved is $J=5\frac{1}{2}\leftarrow 4\frac{1}{2}$ in the $\Omega=7/2$ spin component. The lambda doubling can be clearly seen.

In the case of the far-infrared LMR spectrum of FeH, a

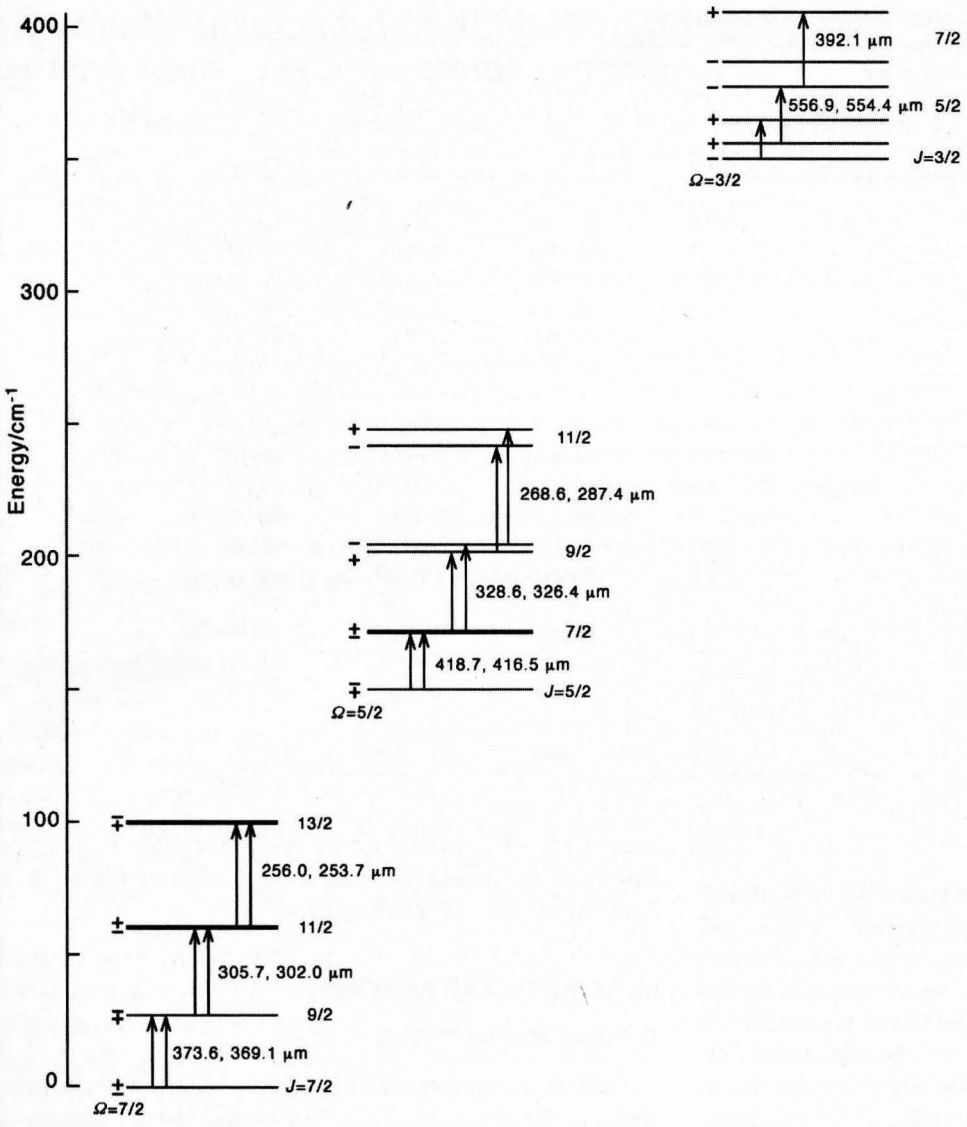

FIG. 1. The lower energy levels of the FeD radical in the $v=0$ level of the $X\,^4\Delta$ state and the transitions involved in the observed far-infrared LMR spectrum. The lambda-type (parity) doubling has been exaggerated by a factor of 100 for the sake of clarity. All the transitions observed obey the selection rule $\Delta J=+1$, $\pm \leftarrow \mp$.

small proton hyperfine splitting was just resolvable.[10] The corresponding splitting was not observed in the spectra of FeD; this is to be expected since the magnetic dipole moment of the deuteron is 6.5 times smaller. The dominant isotope of iron is ^{56}Fe (91.7%); the analysis given in the present paper is confined to this isotopologue. Signals from ^{54}FeD (5.8%) were also recorded as can be seen in both Figs. 2 and 3.

B. Assignment of the LMR spectra

The rotational transition for each LMR spectrum was easily assigned by the use of the term values determined by Balfour *et al.*[30] from the electronic spectrum; indeed, the term values were used to select the laser lines for the present experiments. Since these term values go no lower than $J=3\frac{1}{2}$, some extrapolation was needed to reach the actual J values studied. The assignment of the M_J quantum numbers for each individual LMR spectrum was based on the identification of Zeeman patterns, which consist of the relative magnetic fields, relative intensities, and linewidths in mT. In both π ($\Delta M_J=0$) and σ ($\Delta M_J=\pm 1$) polarizations, these patterns are consistent with a linear Zeeman effect

$$h\nu_L = h\nu_0 + (g'_J M'_J - g''_J M''_J)\mu_B B_Z. \quad (1)$$

In this equation, ν_L is the laser frequency, ν_0 is the zero-field transition frequency, g_J is the molecular g-factor, and M_J is the quantum number for the component of the rotational angular momentum J along the direction of the magnetic flux B_Z; the single and double primes are used to distinguish the upper and lower levels involved in the transition, respectively. The LMR spectrum in π polarization is easy to assign because the resonant field is proportional to $1/M_J$ to a good approximation. Because g'_J is less than g''_J for all the transitions studied, the first line in the σ-spectrum falls at a lower field than that in the π-spectrum. Once this resonance has been established, the Zeeman progression with $\Delta M_J=1$ or -1 can be followed through with the help of the formula in Eq. (1). This procedure is relatively easy if the lambda doubling is small; one simply looks for a progression of doublets with the spacing inversely proportional to the resonance field. Once the lambda doubling becomes large compared with the spacing between the M_J components, the assignment is more challenging.

The measurements of the individual resonances, together with their assignments, are given in Table II. All the transi-

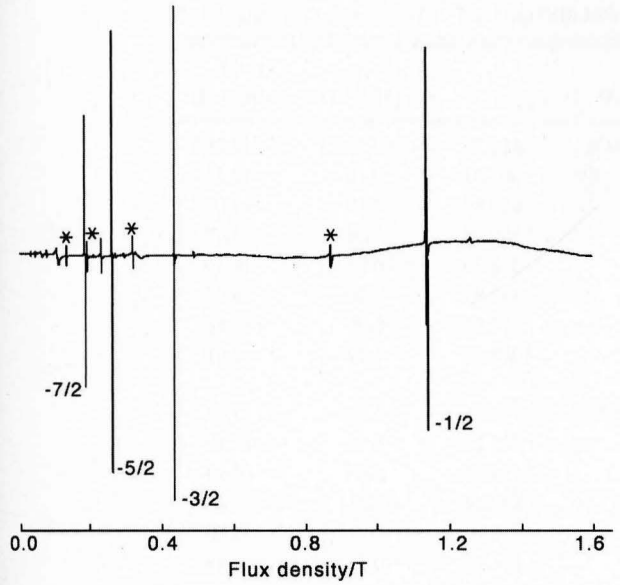

FIG. 2. Part of the far-infrared LMR spectrum of the FeD radical in the $v=0$ level of the $X\,^4\Delta$ state. The spectrum is recorded with the 369.1 μm laser line in parallel polarization ($\Delta M_J=0$). The pure rotational transitions involved are $J=4\frac{1}{2}\leftarrow 3\frac{1}{2}$, $\Omega=7/2$; the values for the quantum number M_J are marked by the resonances. On closer inspection, each resonance shows a small doublet structure caused by lambda-type doubling. The corresponding resonances for ^{54}FeD (5.8%) can also be identified, marked by asterisks.

tions detected are electric dipole in character and obey the parity selection rule, $+\leftrightarrow-$. The absolute parities assigned to the levels of FeD in this work are taken from those derived for FeH.[21]

C. Analysis of the data

As explained in the previous paper[10] on the far-infrared LMR spectrum of the FeH radical, it is not possible to analyze the measurements of FeD in terms of an effective Hamiltonian[27] because of a major breakdown in the Born–Oppenheimer approximation. We have therefore adopted a phenomenological approach to the analysis of the far-infrared LMR spectra. Each individual spin-rotational energy level is described by the formula

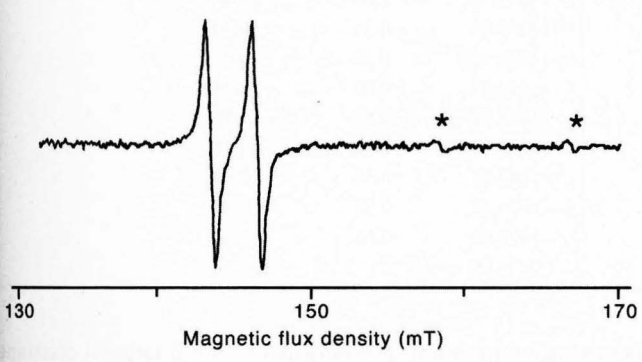

FIG. 3. A small portion of the far-infrared LMR spectrum of the FeD radical in the $v=0$ level of the $X\,^4\Delta$ state, recorded with the 302.0 μm laser line in perpendicular polarization ($\Delta M_J=\pm 1$). The transitions involved are $\Omega=7/2$, $J=5\frac{1}{2}\leftarrow 4\frac{1}{2}$, and $M_J=1\frac{1}{2}\leftarrow\frac{1}{2}$. The well-resolved doublet structure arises from lambda-type doubling. The two weak resonances at higher field, marked by asterisks, can be assigned to a different M_J transition of ^{54}FeD (5.8%) with a slower tuning rate.

$$E_{J,\Omega,\mathrm{par}}(M_j)=E_0+g_J\mu_B B_Z M_J+c_1\mu_B^2 B_Z^2+c_2\mu_B^2 B_Z^2 M_J^2, \tag{2}$$

where E_0 is the zero-field energy of a level characterized by its J, Ω, and parity values. The second term on the right hand side describes the dominant linear Zeeman effect in terms of a Landé-type g-factor. The third and fourth terms on the right hand side model the second-order Zeeman effect arising from the admixture of adjacent rotational levels; these terms are expected to be smaller than the linear effect. The formula given in Eq. (2) can be regarded as an extension of that given in Eq. (1). As explained in Ref. 10, when modeling the energy levels with the formula in Eq. (2), it is desirable to record the LMR spectra associated with each rotational transition of FeD on at least two different laser lines. It can be seen from Table I that this has been possible in almost all cases.

Once the individual LMR spectra had been assigned, a global fit of all the data for the three lowest spin components ($\Omega=7/2$, 5/2, and 3/2) for FeD was carried out by linear least squares to determine values for the parameters E_0, g_J, c_1, and c_2 in Eq. (2) for each rotational level involved; the lowest rotational level ($J=3\frac{1}{2}$, $\Omega=7/2$, parity=$-$) was taken as the zero of energy in the fit. In the case of FeD, it has not yet proved possible to detect fine-structure transitions between the different spin components. Consequently, the data break down into six unconnected sets, three for each spin component multiplied by 2 for the e and f levels. In order to generate a single set of energy levels, we have included the required lambda doubling and spin-orbit intervals, constrained to values determined from experimental data, as data points in the fit. The lambda-doubling interval $\Delta\nu_\Omega$, equal to $\Delta\nu_\Omega=(E_f-E_e)$, for each spin component of the $^4\Delta$ state has been modeled as follows:[35]

$$\Delta\nu_{7/2}=k_{7/2}\left[\left(J+\tfrac{1}{2}\right)^2-9\right]\left[\left(J+\tfrac{1}{2}\right)^2-4\right]\left[\left(J+\tfrac{1}{2}\right)^2-1\right]\left(J+\tfrac{1}{2}\right), \tag{3}$$

$$\Delta\nu_{5/2}=k_{5/2}\left[\left(J+\tfrac{1}{2}\right)^2-4\right]\left[\left(J+\tfrac{1}{2}\right)^2-1\right]\left(J+\tfrac{1}{2}\right), \tag{4}$$

$$\Delta\nu_{3/2}=k_{3/2}\left[\left(J+\tfrac{1}{2}\right)^2-1\right]\left(J+\tfrac{1}{2}\right). \tag{5}$$

The lambda doubling observed in the $R_{7/2}(3\frac{1}{2})$ spectrum was determined in a least-squares fit of the data to be 7.00(53) MHz. This splitting corresponds to 35 280$k_{7/2}$ [the difference between the values for $J=4\frac{1}{2}$ and $3\frac{1}{2}$ in Eq. (3)]; from this, we calculate that the lambda doubling in the $J=3\frac{1}{2}$ level is 1.009 MHz. The separation between the two parity levels of the $J=3\frac{1}{2}$ level was constrained to this value in the global fit of all the LMR data. The corresponding lambda-doubling intervals for the $\Omega=5/2$ and 3/2 components are 35.77 MHz ($J=2\frac{1}{2}$) and 1 429.01 MHz ($J=1\frac{1}{2}$), respectively. The procedure for estimating the fine-structure intervals is described in Sec. IV. The separation between the $J=2\frac{1}{2}$, $\Omega=5/2$, parity=+ and $J=3\frac{1}{2}$, $\Omega=7/2$, parity=$-$ levels was constrained to 4482.1996 GHz and that between $J=1\frac{1}{2}$, $\Omega=3/2$, parity=$-$ and $J=2\frac{1}{2}$, $\Omega=5/2$, parity=+ levels was constrained to 5992.1061 GHz.

TABLE II. Measurements and assignments of the far-infrared LMR spectrum of FeD in the $X\,^4\Delta$ state.

$J' \leftarrow J''$	Ω	Parity	$M_J' \leftarrow M_J''$	ν_L (GHz)	B_Z (mT)	$\nu_L - \nu_{calc}$ (MHz)	$\partial\nu/\partial B_Z$ (MHz/mT)
$4\frac{1}{2}\leftarrow 3\frac{1}{2}$	7/2	$+\leftarrow -$	$3\frac{1}{2}\leftarrow 3\frac{1}{2}$	802.4928	355.56	−0.21	−17.79
			$2\frac{1}{2}\leftarrow 2\frac{1}{2}$		501.51	−0.10	−12.52
			$1\frac{1}{2}\leftarrow 1\frac{1}{2}$		860.62	4.19	−7.08
			$1\frac{1}{2}\leftarrow 2\frac{1}{2}$		259.17	0.04	−24.35
			$\frac{1}{2}\leftarrow 1\frac{1}{2}$		328.20	0.85	−19.16
			$-\frac{1}{2}\leftarrow \frac{1}{2}$		447.87	−0.00	−13.95
			$-1\frac{1}{2}\leftarrow -\frac{1}{2}$		707.04	−0.06	−8.68
			$4\frac{1}{2}\leftarrow 3\frac{1}{2}$		1044.81	−1.19	−6.01
$4\frac{1}{2}\leftarrow 3\frac{1}{2}$	7/2	$+\leftarrow -$	$-3\frac{1}{2}\leftarrow -3\frac{1}{2}$	812.1954	190.21	−0.40	17.77
			$-2\frac{1}{2}\leftarrow -2\frac{1}{2}$		265.28	−0.75	12.79
			$-1\frac{1}{2}\leftarrow -1\frac{1}{2}$		435.95	0.08	7.89
			$-\frac{1}{2}\leftarrow -\frac{1}{2}$		1139.94	−2.21	3.40
			$-1\frac{1}{2}\leftarrow -2\frac{1}{2}$		138.10	1.31	24.50
			$-\frac{1}{2}\leftarrow -1\frac{1}{2}$		174.10	−0.33	19.47
			$\frac{1}{2}\leftarrow -\frac{1}{2}$		235.28	−1.36	14.46
			$1\frac{1}{2}\leftarrow \frac{1}{2}$		362.06	−1.76	9.48
			$-4\frac{1}{2}\leftarrow -3\frac{1}{2}$		561.10	2.13	6.01
			$2\frac{1}{2}\leftarrow 1\frac{1}{2}$		773.90	2.03	4.60
$4\frac{1}{2}\leftarrow 3\frac{1}{2}$	7/2	$-\leftarrow +$	$3\frac{1}{2}\leftarrow 3\frac{1}{2}$	802.4928	355.94	−0.40	−17.79
			$2\frac{1}{2}\leftarrow 2\frac{1}{2}$		502.02	−0.65	−12.52
			$1\frac{1}{2}\leftarrow 1\frac{1}{2}$		861.52	3.68	−7.08
			$1\frac{1}{2}\leftarrow 2\frac{1}{2}$		259.45	−0.18	−24.35
			$\frac{1}{2}\leftarrow 1\frac{1}{2}$		328.54	−1.38	−19.16
			$-\frac{1}{2}\leftarrow \frac{1}{2}$		448.40	0.34	−13.95
			$-1\frac{1}{2}\leftarrow -\frac{1}{2}$		707.83	−0.74	−8.68
			$4\frac{1}{2}\leftarrow 3\frac{1}{2}$		1045.89	−0.90	−6.07
$4\frac{1}{2}\leftarrow 3\frac{1}{2}$	7/2	$-\leftarrow +$	$-3\frac{1}{2}\leftarrow -3\frac{1}{2}$	812.1954	189.83	−0.38	17.77
			$-2\frac{1}{2}\leftarrow -2\frac{1}{2}$		264.77	−0.95	12.79
			$-1\frac{1}{2}\leftarrow -1\frac{1}{2}$		435.11	−0.00	7.89
			$-\frac{1}{2}\leftarrow -\frac{1}{2}$		1137.94	−1.96	3.39
			$-1\frac{1}{2}\leftarrow -2\frac{1}{2}$		137.84	0.83	24.50
			$-\frac{1}{2}\leftarrow -1\frac{1}{2}$		173.76	−0.59	19.47
			$\frac{1}{2}\leftarrow -\frac{1}{2}$		234.82	−1.63	14.46
			$1\frac{1}{2}\leftarrow \frac{1}{2}$		360.96	1.65	9.48
			$-4\frac{1}{2}\leftarrow -3\frac{1}{2}$		560.12	1.88	6.01
			$2\frac{1}{2}\leftarrow 1\frac{1}{2}$		772.47	1.40	4.60
$5\frac{1}{2}\leftarrow 4\frac{1}{2}$	7/2	$-\leftarrow +$	$4\frac{1}{2}\leftarrow 4\frac{1}{2}$	980.5916	887.74	1.63	−12.34
			$3\frac{1}{2}\leftarrow 3\frac{1}{2}$		1147.05	−0.13	−9.50
			$2\frac{1}{2}\leftarrow 2\frac{1}{2}$		1626.34	−1.26	−6.61
			$3\frac{1}{2}\leftarrow 4\frac{1}{2}$		514.47	−0.06	−21.34
			$2\frac{1}{2}\leftarrow 3\frac{1}{2}$		591.32	−0.56	−18.55
			$1\frac{1}{2}\leftarrow 2\frac{1}{2}$		695.31	0.03	−15.75
			$\frac{1}{2}\leftarrow 1\frac{1}{2}$		843.75	−0.39	−12.94
			$-\frac{1}{2}\leftarrow \frac{1}{2}$		1073.46	0.94	−10.13
			$-1\frac{1}{2}\leftarrow -\frac{1}{2}$		1476.69	0.64	−7.30

The information in each LMR spectrum depends on the difference in the values of the second-order Zeeman parameter c_1, not their separate values. In the absence of any information on the fine-structure transitions, the parameter c_1 had therefore to be estimated for the lowest level of each Ω and parity set. Since this parameter arises from the effect of magnetic-field mixing of adjacent rotational levels, it is expected to be inversely proportional to the rotational constant B from second-order perturbation theory. We have therefore estimated the c_1 values from those determined for FeH,[10] scaling in the ratio of the B values for each Ω component. The values used in the FeD fit were as follows:

$\Omega = 7/2$, $J = 3\frac{1}{2}$, parity $= \pm$ $\quad c_1 = 0.0$,

TABLE II. (*Continued.*)

$J' \leftarrow J''$	Ω	Parity	$M_J' \leftarrow M_J''$	ν_L (GHz)	B_Z (mT)	$\nu_L - \nu_{\text{calc}}$ (MHz)	$\partial\nu/\partial B_Z$ (MHz/mT)
$5\frac{1}{2} \leftarrow 4\frac{1}{2}$	7/2	$- \leftarrow +$	$-4\frac{1}{2} \leftarrow -4\frac{1}{2}$	992.7089	89.81	0.28	12.45
			$-3\frac{1}{2} \leftarrow -3\frac{1}{2}$		115.46	−0.19	9.69
			$-2\frac{1}{2} \leftarrow -2\frac{1}{2}$		161.37	0.33	6.94
			$-1\frac{1}{2} \leftarrow -1\frac{1}{2}$		267.98	−0.60	4.20
			$-\frac{1}{2} \leftarrow -\frac{1}{2}$		763.03	0.73	1.55
			$-3\frac{1}{2} \leftarrow -4\frac{1}{2}$		52.17	0.27	21.43
			$-2\frac{1}{2} \leftarrow -3\frac{1}{2}$		59.90	0.16	18.67
			$-1\frac{1}{2} \leftarrow -2\frac{1}{2}$		70.32	−0.01	15.91
			$-\frac{1}{2} \leftarrow -1\frac{1}{2}$		85.10	−0.11	13.15
			$\frac{1}{2} \leftarrow -\frac{1}{2}$		107.85	−0.84	10.39
			$1\frac{1}{2} \leftarrow \frac{1}{2}$		146.86	−0.00	7.63
			$2\frac{1}{2} \leftarrow 1\frac{1}{2}$		230.38	−0.24	4.87
			$-5\frac{1}{2} \leftarrow -4\frac{1}{2}$		322.55	−0.47	3.48
			$3\frac{1}{2} \leftarrow 2\frac{1}{2}$		530.76	−0.40	2.15
$5\frac{1}{2} \leftarrow 4\frac{1}{2}$	7/2	$+ \leftarrow -$	$4\frac{1}{2} \leftarrow 4\frac{1}{2}$	980.5916	889.49	1.29	−12.35
			$3\frac{1}{2} \leftarrow 3\frac{1}{2}$		1149.36	−0.03	−9.50
			$2\frac{1}{2} \leftarrow 2\frac{1}{2}$		1629.62	−1.22	−6.61
			$3\frac{1}{2} \leftarrow 4\frac{1}{2}$		515.52	−0.19	−21.34
			$2\frac{1}{2} \leftarrow 3\frac{1}{2}$		592.60	0.55	−18.55
			$1\frac{1}{2} \leftarrow 2\frac{1}{2}$		696.77	0.25	−15.75
			$\frac{1}{2} \leftarrow 1\frac{1}{2}$		845.55	−0.08	−12.94
			$-\frac{1}{2} \leftarrow \frac{1}{2}$		1075.75	0.75	−10.13
			$-1\frac{1}{2} \leftarrow -\frac{1}{2}$		1479.99	0.49	−7.30
$5\frac{1}{2} \leftarrow 4\frac{1}{2}$	7/2	$+ \leftarrow -$	$-4\frac{1}{2} \leftarrow -4\frac{1}{2}$	992.7089	87.94	0.16	12.45
			$-3\frac{1}{2} \leftarrow -3\frac{1}{2}$		113.05	−0.24	9.69
			$-2\frac{1}{2} \leftarrow -2\frac{1}{2}$		157.99	0.38	6.94
			$-1\frac{1}{2} \leftarrow -1\frac{1}{2}$		292.38	−0.48	4.20
			$-\frac{1}{2} \leftarrow -\frac{1}{2}$		747.90	0.77	1.54
			$-3\frac{1}{2} \leftarrow -4\frac{1}{2}$		51.07	0.48	21.43
			$-2\frac{1}{2} \leftarrow -3\frac{1}{2}$		58.67	−0.23	18.67
			$-1\frac{1}{2} \leftarrow -2\frac{1}{2}$		68.85	0.03	15.91
			$-\frac{1}{2} \leftarrow -1\frac{1}{2}$		83.36	−0.35	13.15
			$\frac{1}{2} \leftarrow -\frac{1}{2}$		105.59	−0.68	10.39
			$1\frac{1}{2} \leftarrow \frac{1}{2}$		143.81	−0.02	7.63
			$2\frac{1}{2} \leftarrow 1\frac{1}{2}$		225.64	−0.36	4.87
			$-5\frac{1}{2} \leftarrow -4\frac{1}{2}$		315.68	−0.37	3.48
			$3\frac{1}{2} \leftarrow 2\frac{1}{2}$		520.24	−0.90	2.15
$6\frac{1}{2} \leftarrow 5\frac{1}{2}$	7/2	$+ \leftarrow -$	$5\frac{1}{2} \leftarrow 5\frac{1}{2}$	1170.9410	527.28	1.73	−9.21
			$4\frac{1}{2} \leftarrow 4\frac{1}{2}$		644.95	1.08	−7.52
			$3\frac{1}{2} \leftarrow 3\frac{1}{2}$		830.55	0.14	−5.83
			$2\frac{1}{2} \leftarrow 2\frac{1}{2}$		1167.26	−2.51	−4.13
			$4\frac{1}{2} \leftarrow 5\frac{1}{2}$		294.42	−0.93	−16.52
			$3\frac{1}{2} \leftarrow 4\frac{1}{2}$		327.83	−0.41	−14.84
			$2\frac{1}{2} \leftarrow 3\frac{1}{2}$		369.81	0.38	−13.15
			$1\frac{1}{2} \leftarrow 2\frac{1}{2}$		424.00	−0.12	−11.47
			$\frac{1}{2} \leftarrow 1\frac{1}{2}$		496.81	−0.91	−9.79
			$-\frac{1}{2} \leftarrow \frac{1}{2}$		600.06	−0.48	−8.10
			$-1\frac{1}{2} \leftarrow -\frac{1}{2}$		757.59	−0.623	−6.41
			$-2\frac{1}{2} \leftarrow -1\frac{1}{2}$		1028.00	0.62	−4.71
			$-3\frac{1}{2} \leftarrow -2\frac{1}{2}$		1601.80	−0.48	−3.00

$\Omega = 5/2,\ J = 2\frac{1}{2},\ \text{parity} = +\quad c_1 = 0.7681 \times 10^{-3}\ \text{GHz}^{-1},$

$\Omega = 5/2,\ J = 2\frac{1}{2},\ \text{parity} = -\quad c_1 = 0.7606 \times 10^{-3}\ \text{GHz}^{-1},$

$\Omega = 3/2,\ J = 1\frac{1}{2},\ \text{parity} = -\quad c_1 = 0.2451 \times 10^{-2}\ \text{GHz}^{-1},$

$\Omega = 3/2,\ J = 1\frac{1}{2},\ \text{parity} = +\quad c_1 = 0.2193 \times 10^{-2}\ \text{GHz}^{-1}.$

TABLE II. (*Continued.*)

$J' \leftarrow J''$	Ω	Parity	$M_J' \leftarrow M_J''$	ν_L (GHz)	B_Z (mT)	$\nu_L - \nu_{\text{calc}}$ (MHz)	$\partial\nu/\partial B_Z$ (MHz/mT)
$6\frac{1}{2} \leftarrow 5\frac{1}{2}$	7/2	$+ \leftarrow -$	$-5\frac{1}{2} \leftarrow -5\frac{1}{2}$	1181.5889	620.54	−1.49	9.35
			$-4\frac{1}{2} \leftarrow -4\frac{1}{2}$		757.27	1.38	7.66
			$-3\frac{1}{2} \leftarrow -3\frac{1}{2}$		971.98	−0.70	5.99
			$-2\frac{1}{2} \leftarrow -2\frac{1}{2}$		1353.50	1.68	4.32
			$-3\frac{1}{2} \leftarrow -4\frac{1}{2}$		387.47	−0.57	14.94
			$-2\frac{1}{2} \leftarrow -3\frac{1}{2}$		436.91	−0.18	13.25
			$-1\frac{1}{2} \leftarrow -2\frac{1}{2}$		500.83	−0.07	11.56
			$-\frac{1}{2} \leftarrow -1\frac{1}{2}$		586.55	0.81	9.87
			$\frac{1}{2} \leftarrow -\frac{1}{2}$		707.77	0.59	8.18
			$1\frac{1}{2} \leftarrow \frac{1}{2}$		891.86	0.65	6.50
$6\frac{1}{2} \leftarrow 5\frac{1}{2}$	7/2	$- \leftarrow +$	$5\frac{1}{2} \leftarrow 5\frac{1}{2}$	1170.9410	533.88	1.65	−9.22
			$4\frac{1}{2} \leftarrow 4\frac{1}{2}$		653.07	1.26	−7.53
			$3\frac{1}{2} \leftarrow 3\frac{1}{2}$		841.04	0.35	−5.83
			$2\frac{1}{2} \leftarrow 2\frac{1}{2}$		1181.96	−2.88	−4.13
			$4\frac{1}{2} \leftarrow 5\frac{1}{2}$		298.16	−1.31	−16.52
			$3\frac{1}{2} \leftarrow 4\frac{1}{2}$		332.03	−0.39	−14.84
			$2\frac{1}{2} \leftarrow 3\frac{1}{2}$		374.49	−0.53	−13.15
			$1\frac{1}{2} \leftarrow 2\frac{1}{2}$		429.39	−0.97	−11.47
			$\frac{1}{2} \leftarrow 1\frac{1}{2}$		503.48	1.40	−9.78
			$-\frac{1}{2} \leftarrow \frac{1}{2}$		607.99	0.41	−8.10
			$-1\frac{1}{2} \leftarrow -\frac{1}{2}$		767.41	−1.15	−6.41
			$-2\frac{1}{2} \leftarrow -1\frac{1}{2}$		1041.72	0.64	−4.71
			$-3\frac{1}{2} \leftarrow -2\frac{1}{2}$		1623.77	−0.35	−3.00
$6\frac{1}{2} \leftarrow 5\frac{1}{2}$	7/2	$- \leftarrow +$	$-5\frac{1}{2} \leftarrow -5\frac{1}{2}$	1181.5889	613.70	−1.11	9.35
			$-4\frac{1}{2} \leftarrow -4\frac{1}{2}$		749.13	0.18	7.66
			$-3\frac{1}{2} \leftarrow -3\frac{1}{2}$		961.20	0.17	5.98
			$-2\frac{1}{2} \leftarrow -2\frac{1}{2}$		1338.78	1.44	4.32
			$-3\frac{1}{2} \leftarrow -4\frac{1}{2}$		383.25	−0.70	14.93
			$-2\frac{1}{2} \leftarrow -3\frac{1}{2}$		432.11	0.31	13.25
			$-1\frac{1}{2} \leftarrow -2\frac{1}{2}$		495.38	−0.09	11.56
			$-\frac{1}{2} \leftarrow -1\frac{1}{2}$		580.24	0.22	9.87
			$\frac{1}{2} \leftarrow -\frac{1}{2}$		700.20	−0.11	8.18
			$1\frac{1}{2} \leftarrow \frac{1}{2}$		882.14	1.46	6.50
$3\frac{1}{2} \leftarrow 2\frac{1}{2}$	5/2	$- \leftarrow +$	$-2\frac{1}{2} \leftarrow -2\frac{1}{2}$	719.7511	316.73	1.55	15.27
			$-1\frac{1}{2} \leftarrow -1\frac{1}{2}$		521.15	−1.93	9.41
			$-\frac{1}{2} \leftarrow -\frac{1}{2}$		1364.90	−0.35	4.03
			$-\frac{1}{2} \leftarrow -1\frac{1}{2}$		273.98	1.31	17.70
			$\frac{1}{2} \leftarrow -\frac{1}{2}$		415.95	1.26	11.76
			$-3\frac{1}{2} \leftarrow -2\frac{1}{2}$		707.95	−0.05	6.84
			$1\frac{1}{2} \leftarrow \frac{1}{2}$		852.60	1.14	5.96
$3\frac{1}{2} \leftarrow 2\frac{1}{2}$	5/2	$- \leftarrow +$	$-2\frac{1}{2} \leftarrow -2\frac{1}{2}$	715.9876	69.96	0.66	15.23
			$-1\frac{1}{2} \leftarrow -1\frac{1}{2}$		116.34	−0.21	9.19
			$-\frac{1}{2} \leftarrow -\frac{1}{2}$		336.69	−0.17	3.29
			$-\frac{1}{2} \leftarrow -1\frac{1}{2}$		6.70	−0.36	17.58
			$\frac{1}{2} \leftarrow -\frac{1}{2}$		92.86	−1.43	11.52
			$-3\frac{1}{2} \leftarrow -2\frac{1}{2}$		156.49	0.43	6.81
			$1\frac{1}{2} \leftarrow \frac{1}{2}$		196.29	−1.83	5.50

Each data point in the fit was assigned the same weight, consistent with an experimental uncertainty in the measurement of 2 MHz. The standard deviation of the fit of 239 data relative to experimental uncertainty was 0.545, which suggests that the estimate of experimental uncertainty is somewhat conservative. The values for the various parameters determined in the least-squares fit are listed in Table III, together with their estimated uncertainties. The residuals from this fit are given in Table II. Two data points in the 268.8 μm spectrum (π polarization) were zero weighted in

TABLE II. (*Continued.*)

$J' \leftarrow J''$	Ω	Parity	$M_J' \leftarrow M_J''$	ν_L (GHz)	B_Z (mT)	$\nu_L - \nu_{calc}$ (MHz)	$\partial\nu/\partial B_Z$ (MHz/mT)
$3\frac{1}{2} \leftarrow 2\frac{1}{2}$	5/2	+ ← −	$-2\frac{1}{2} \leftarrow -2\frac{1}{2}$	719.7511	304.73	2.05	15.28
			$-1\frac{1}{2} \leftarrow -1\frac{1}{2}$		501.55	−0.00	9.41
			$-\frac{1}{2} \leftarrow -\frac{1}{2}$		1320.30	−0.79	4.00
			$-\frac{1}{2} \leftarrow -1\frac{1}{2}$		263.83	1.28	17.70
			$\frac{1}{2} \leftarrow -\frac{1}{2}$		400.85	0.80	11.74
			$-3\frac{1}{2} \leftarrow -2\frac{1}{2}$		680.20	−0.47	6.86
			$1\frac{1}{2} \leftarrow \frac{1}{2}$		823.50	1.98	5.93
$3\frac{1}{2} \leftarrow 2\frac{1}{2}$	5/2	+ ← −	$-2\frac{1}{2} \leftarrow -2\frac{1}{2}$	715.9876	58.17	0.42	15.24
			$-1\frac{1}{2} \leftarrow -1\frac{1}{2}$		96.85	−0.91	9.19
			$-\frac{1}{2} \leftarrow -1\frac{1}{2}$		281.96	−0.95	3.25
			$\frac{1}{2} \leftarrow -\frac{1}{2}$		77.31	−1.25	11.51
			$-3\frac{1}{2} \leftarrow -2\frac{1}{2}$		129.96	−0.02	6.82
			$1\frac{1}{2} \leftarrow \frac{1}{2}$		163.95	−2.13	5.48
$4\frac{1}{2} \leftarrow 3\frac{1}{2}$	5/2	+ ← −	$3\frac{1}{2} \leftarrow 3\frac{1}{2}$	912.3739	546.30	0.87	−9.54
			$2\frac{1}{2} \leftarrow 2\frac{1}{2}$		767.58	0.21	−6.76
			$1\frac{1}{2} \leftarrow 1\frac{1}{2}$		1296.94	−0.84	−3.95
			$2\frac{1}{2} \leftarrow 3\frac{1}{2}$		343.59	1.12	−15.20
			$1\frac{1}{2} \leftarrow 2\frac{1}{2}$		419.26	0.61	−12.45
			$\frac{1}{2} \leftarrow 1\frac{1}{2}$		537.77	−0.12	−9.70
			$-\frac{1}{2} \leftarrow \frac{1}{2}$		750.25	−0.07	−6.93
			$-1\frac{1}{2} \leftarrow -\frac{1}{2}$		1243.57	0.07	−4.15
			$4\frac{1}{2} \leftarrow 3\frac{1}{2}$		1328.44	−0.11	−3.99
$4\frac{1}{2} \leftarrow 3\frac{1}{2}$	5/2	+ ← −	$-3\frac{1}{2} \leftarrow -3\frac{1}{2}$	918.4170	83.29	−0.86	9.66
			$-2\frac{1}{2} \leftarrow -2\frac{1}{2}$		116.54	−0.86	6.91
			$-1\frac{1}{2} \leftarrow -1\frac{1}{2}$		193.84	−0.86	4.16
			$-\frac{1}{2} \leftarrow -1\frac{1}{2}$		82.07	−0.71	9.80
			$\frac{1}{2} \leftarrow -\frac{1}{2}$		114.15	−0.54	7.05
			$1\frac{1}{2} \leftarrow \frac{1}{2}$		187.39	−0.38	4.30
			$-4\frac{1}{2} \leftarrow -3\frac{1}{2}$		200.94	0.89	4.00
$4\frac{1}{2} \leftarrow 3\frac{1}{2}$	5/2	− ← +	$3\frac{1}{2} \leftarrow 3\frac{1}{2}$	912.3739	598.44	1.02	−9.55
			$2\frac{1}{2} \leftarrow 2\frac{1}{2}$		840.99	0.34	−6.77
			$1\frac{1}{2} \leftarrow 1\frac{1}{2}$		1421.84	−1.08	−3.94
			$2\frac{1}{2} \leftarrow 3\frac{1}{2}$		376.90	1.02	−15.21
			$1\frac{1}{2} \leftarrow 2\frac{1}{2}$		460.11	0.91	−12.45
			$\frac{1}{2} \leftarrow 1\frac{1}{2}$		590.51	0.10	−9.69
			$-\frac{1}{2} \leftarrow \frac{1}{2}$		824.67	−0.15	−6.92
			$-1\frac{1}{2} \leftarrow -\frac{1}{2}$		1370.63	0.87	−4.13
			$4\frac{1}{2} \leftarrow 3\frac{1}{2}$		1447.22	−0.13	−3.92
$4\frac{1}{2} \leftarrow 3\frac{1}{2}$	5/2	− ← +	$-1\frac{1}{2} \leftarrow -1\frac{1}{2}$	918.4170	70.62	−0.56	4.15
			$-\frac{1}{2} \leftarrow -1\frac{1}{2}$		210.33	−0.97	1.41
			$-1\frac{1}{2} \leftarrow -2\frac{1}{2}$		23.25	0.53	12.56
			$-\frac{1}{2} \leftarrow -1\frac{1}{2}$		29.79	0.72	9.79
			$1\frac{1}{2} \leftarrow \frac{1}{2}$		68.79	−1.16	4.27
			$-4\frac{1}{2} \leftarrow -3\frac{1}{2}$		73.01	−1.49	4.03
$5\frac{1}{2} \leftarrow 4\frac{1}{2}$	5/2	− ← +	$4\frac{1}{2} \leftarrow 4\frac{1}{2}$	1116.2450	461.20	0.18	−6.55
			$3\frac{1}{2} \leftarrow 3\frac{1}{2}$		593.31	0.13	−5.09
			$2\frac{1}{2} \leftarrow 3\frac{1}{2}$		326.30	−0.13	−9.28
			$1\frac{1}{2} \leftarrow 2\frac{1}{2}$		387.26	−0.11	−7.83
			$\frac{1}{2} \leftarrow 1\frac{1}{2}$		476.24	−0.08	−6.37
			$-\frac{1}{2} \leftarrow \frac{1}{2}$		618.25	−0.46	−4.90
			$-1\frac{1}{2} \leftarrow -\frac{1}{2}$		881.34	−0.24	−3.44

TABLE II. (*Continued.*)

$J' \leftarrow J''$	Ω	Parity	$M_J' \leftarrow M_J''$	ν_L (GHz)	B_Z (mT)	$\nu_L - \nu_{\text{calc}}$ (MHz)	$\partial\nu/\partial B_Z$ (MHz/mT)
$5\frac{1}{2} \leftarrow 4\frac{1}{2}$	5/2	$- \leftarrow +$	$-4\frac{1}{2} \leftarrow -4\frac{1}{2}$	1120.9577	252.25	0.00	6.66
			$-3\frac{1}{2} \leftarrow -3\frac{1}{2}$		324.30	−0.41	5.18
			$-2\frac{1}{2} \leftarrow -2\frac{1}{2}$		453.48	0.30	3.71
			$-1\frac{1}{2} \leftarrow -1\frac{1}{2}$		753.51	0.76	2.24
			$-3\frac{1}{2} \leftarrow -4\frac{1}{2}$		154.67	0.58	10.84
			$-2\frac{1}{2} \leftarrow -3\frac{1}{2}$		179.11	0.15	9.36
			$-1\frac{1}{2} \leftarrow -2\frac{1}{2}$		212.65	0.12	7.89
			$-\frac{1}{2} \leftarrow -1\frac{1}{2}$		261.69	−0.22	6.41
			$\frac{1}{2} \leftarrow -\frac{1}{2}$		340.01	−0.23	4.93
			$1\frac{1}{2} \leftarrow \frac{1}{2}$		485.19	−0.23	3.45
			$-5\frac{1}{2} \leftarrow -4\frac{1}{2}$		683.21	−0.12	2.47
$5\frac{1}{2} \leftarrow 4\frac{1}{2}$	5/2	$+ \leftarrow -$	$4\frac{1}{2} \leftarrow 4\frac{1}{2}$	1116.2450	628.47	0.11	−6.57
			$3\frac{1}{2} \leftarrow 4\frac{1}{2}$		385.48	0.25	−10.74
			$2\frac{1}{2} \leftarrow 3\frac{1}{2}$		446.33	−0.18	−9.28
			$1\frac{1}{2} \leftarrow 2\frac{1}{2}$		530.06	−0.27	−7.82
			$\frac{1}{2} \leftarrow 1\frac{1}{2}$		652.56	0.15	−6.35
			$-\frac{1}{2} \leftarrow \frac{1}{2}$		848.58	0.07	−4.89
$5\frac{1}{2} \leftarrow 4\frac{1}{2}$	5/2	$+ \leftarrow -$	$-2\frac{1}{2} \leftarrow -2\frac{1}{2}$	1120.9577	214.87[a]	−240.21	3.71
			$-1\frac{1}{2} \leftarrow -1\frac{1}{2}$		358.62[a]	−242.62	2.23
			$1\frac{1}{2} \leftarrow \frac{1}{2}$		162.40	0.08	3.43
			$2\frac{1}{2} \leftarrow 1\frac{1}{2}$		286.24	−0.41	1.94
			$-5\frac{1}{2} \leftarrow -4\frac{1}{2}$		222.54	0.44	2.50
			$-4\frac{1}{2} \leftarrow -3\frac{1}{2}$		546.55	−0.23	1.02
$2\frac{1}{2} \leftarrow 1\frac{1}{2}$	3/2	$+ \leftarrow -$	$-1\frac{1}{2} \leftarrow -1\frac{1}{2}$	540.7831	466.50	0.72	8.14
			$-\frac{1}{2} \leftarrow -\frac{1}{2}$		1291.60	−0.12	3.17
			$-\frac{1}{2} \leftarrow -1\frac{1}{2}$		319.88	−0.57	11.86
			$\frac{1}{2} \leftarrow -\frac{1}{2}$		580.10	0.12	6.62
			$-2\frac{1}{2} \leftarrow -1\frac{1}{2}$		867.22	−0.16	4.39
$2\frac{1}{2} \leftarrow 1\frac{1}{2}$	3/2	$+ \leftarrow -$	$-1\frac{1}{2} \leftarrow -1\frac{1}{2}$	538.3473	166.38	0.35	8.08
			$-\frac{1}{2} \leftarrow -\frac{1}{2}$		483.90	0.10	2.86
			$-\frac{1}{2} \leftarrow -1\frac{1}{2}$		113.87	0.25	11.80
			$\frac{1}{2} \leftarrow -\frac{1}{2}$		208.45	−0.89	6.48
			$-2\frac{1}{2} \leftarrow -1\frac{1}{2}$		309.46	0.06	4.35
			$1\frac{1}{2} \leftarrow \frac{1}{2}$		1109.70	0.14	1.38
$2\frac{1}{2} \leftarrow 1\frac{1}{2}$	3/2	$- \leftarrow +$	$1\frac{1}{2} \leftarrow 1\frac{1}{2}$	540.7831	62.425	0.11	−8.13
			$\frac{1}{2} \leftarrow \frac{1}{2}$		189.55	0.15	−2.65
			$\frac{1}{2} \leftarrow 1\frac{1}{2}$		43.41	−0.36	−11.69
			$-\frac{1}{2} \leftarrow \frac{1}{2}$		81.21	0.15	−6.25
			$2\frac{1}{2} \leftarrow 1\frac{1}{2}$		110.88	−0.04	−4.58
$2\frac{1}{2} \leftarrow 1\frac{1}{2}$	3/2	$- \leftarrow +$	$1\frac{1}{2} \leftarrow 1\frac{1}{2}$	538.3473	363.01	0.01	−8.07
			$\frac{1}{2} \leftarrow \frac{1}{2}$		1173.48	−0.00	−2.30
			$-\frac{1}{2} \leftarrow \frac{1}{2}$		475.54	−0.00	−6.11
			$2\frac{1}{2} \leftarrow 1\frac{1}{2}$		645.01	0.00	−4.54

[a]Upper level perturbed. Measurement excluded from the fit.

the fit because they showed much larger residuals, strongly suggesting that the upper levels of these transitions are perturbed.

Two sets of observations in the far-infrared LMR spectrum have been excluded from the global fit. The first of these is the spectrum recorded with the 392.1 μm laser line. Only two resonances were detected, one in π and one in σ polarization; details are given in Table IV. These resonances can be confidently assigned to the higher frequency lambda-doublet $(+ \leftarrow -)$ of the $R(2\frac{1}{2})$ transition in the $\Omega = 3/2$ spin component. The three Zeeman parameters for the lower level in this transition are known from the global fit (Table III).

TABLE III. Values of the parameters determined in the least-squares fit of the LMR data for FeD in the $v=0$ level of the $X\,^4\Delta$ state.

Ω	J	Parity	E (GHz)	g_J	$10^3 c_1$ (GHz^{-1})	$10^4 c_2$ (GHz^{-1})
7/2	$3\frac{1}{2}$	−	0.0000[a]	1.202 032(41)[b]	0.0000[c]	1.622(15)
		+	0.001 009[c]	1.202 006(41)	0.0000[c]	1.642(15)
	$4\frac{1}{2}$	+	808.815 12(35)	0.839 160(30)	1.9572(42)	−0.0313(85)
		−	808.823 13(35)	0.839 152(30)	1.9562(42)	−0.0225(86)
	$5\frac{1}{2}$	−	1800.405 98(45)	0.641 633(26)	2.5091(48)	−0.1652(48)
		+	1800.437 33(45)	0.641 611(26)	2.5074(48)	−0.1580(56)
	$6\frac{1}{2}$	+	2976.218 77(62)	0.521 160(26)	2.6723(61)	−0.1194(54)
		−	2976.313 08(62)	0.521 105(27)	2.6714(61)	−0.1167(54)
5/2	$2\frac{1}{2}$	+	4482.199 60[c]	1.035 87(13)	0.7681[c]	1.84(12)
		−	4482.235 37[c]	1.035 84(14)	0.7606[c]	1.77(14)
	$3\frac{1}{2}$	−	5197.121 75(43)	0.601 066(62)	2.6796(32)	−0.506(41)
		+	5197.336 63(45)	0.600 738(78)	2.6643(35)	−0.527(49)
	$4\frac{1}{2}$	+	6114.735 37(54)	0.404 190(47)	3.0240(46)	−0.394(20)
		−	6115.461 21(55)	0.403 365(58)	2.9934(44)	−0.395(23)
	$5\frac{1}{2}$	−	7234.018 38(73)	0.299 069(51)	3.0892(96)	−0.245(16)
		+	7235.862 44(84)	0.297 643(65)	3.0363(118)	−0.235(19)
3/2	$1\frac{1}{2}$	−	10 474.3057[c]	0.649 11(52)	2.451[c]	1.24(48)
		+	10 475.734.71[c]	0.642 34(77)	2.1934[c]	1.10(116)
	$2\frac{1}{2}$	+	11 011.3100(13)	0.265 85(13)	3.4640(40)	−0.883(109)
		−	11 017.0257(11)	0.254 30(319)	3.1409(71)	−0.824(217)

[a]The energy levels are measured relative to the lower lambda-doublet (− parity) for the $J=3\frac{1}{2}$ level of the $\Omega=7/2$ spin component.
[b]The figures in parentheses are the standard deviations of the least-squares fit, in units of the last quoted decimal place.
[c]Parameter constrained to this value in the fit; see text for details.

The zero-field transition frequency is estimated to be 575.094 GHz (by extrapolation). If this value is assumed to be correct, a fit of the two data points assigned as in Table IV is reasonably satisfactory and gives a g_J' value of 0.107 78(11). This value lies between Hund's case (a) and case (b) values,[36] 0.0952 and 0.1714, respectively. The assignment of the resonance in the σ spectrum to the $M_J=-3\frac{1}{2}\leftarrow-2\frac{1}{2}$ transition implies that there will be two other $\Delta M_J=+1$ resonances at lower field than the observed line (see Table IV). These were not observed but they are calculated to be much weaker (relative intensities of 2 and 6 compared with 42 for the assigned transition). Clearly, more work with lower frequency laser lines is required to measure this rotational transition accurately. The other observation that was not included in the global fit was made with the 513.0 μm laser line (ν_L=584.3882 GHz). A single resonance was detected in π polarization at 1688.5 mT; a frequency-pulling experiment showed that the tuning rate, $\partial\nu/\partial B_Z$, is positive. The extrapolated zero-field frequency of the higher frequency lambda-doublet (−←+) of the $R(1\frac{1}{2})$ transition in the $\Omega=1/2$ spin component is 569.6 GHz. However, this estimated frequency has a large uncertainty, maybe as much as 30 GHz, because the term values of this spin component show marked perturbations.[30] While it is therefore possible that the observed resonance is associated with the $R_{1/2}(1\frac{1}{2})$ transition, much more work is needed to confirm this speculation.

IV. DISCUSSION

Eight pure rotational transitions in three spin components of the FeD radical in the $v=0$ level of the $X\,^4\Delta$ state

TABLE IV. Details of the LMR spectrum of FeD recorded with the 392.1 μm laser line.

Ω	$J'\leftarrow J''$	Parity	$M_J'\leftarrow M_J''$	ν_L (GHz)	B_Z (mT)	$\nu_L-\nu_{\mathrm{calc}}$ (MHz)	$\partial\nu/\partial B_Z$ (MHz/mT)
3/2	$3\frac{1}{2}\leftarrow2\frac{1}{2}$	+←−	$-2\frac{1}{2}\leftarrow-2\frac{1}{2}$	764.6426	1375.00[a]	−9.7	5.87
			$-1\frac{1}{2}\leftarrow-2\frac{1}{2}$		1088.8[b]		7.22
			$-\frac{1}{2}\leftarrow-1\frac{1}{2}$		1540.6[b]		5.21
			$-3\frac{1}{2}\leftarrow-2\frac{1}{2}$		1834.40[a]	5.2	4.61

[a]Observed resonance.
[b]Calculated resonance using ν_0=757.094 GHz, g_J'=0.10778, g_J''=0.2543, c_1'=0.004, c_1''=0.00314, and $c_2''=-0.824\times10^{-4}$.

TABLE V. Transition frequencies of pure rotational transitions of FeD in the $v=0$ level of the $X\,^4\Delta$ state.

			Transition frequency (GHz)	
Ω	J	Parity	Present work	Previous work (Ref. 30)
7/2	$4\frac{1}{2}\leftarrow 3\frac{1}{2}$	$+\leftarrow -$	808.815 12(35)[a]	808.360[b]
		$-\leftarrow +$	808.822 12(35)	808.360[b]
	$5\frac{1}{2}\leftarrow 4\frac{1}{2}$	$-\leftarrow +$	991.590 86(57)	991.444[b]
		$+\leftarrow -$	991.614 20(57)	991.444[b]
	$6\frac{1}{2}\leftarrow 5\frac{1}{2}$	$+\leftarrow -$	1175.812 79(76)	1175.966[b]
		$-\leftarrow +$	1175.875 75(76)	1175.966[b]
5/2	$3\frac{1}{2}\leftarrow 2\frac{1}{2}$	$-\leftarrow +$	714.922 15(43)	714.473[b,c]
		$+\leftarrow -$	715.101 26(45)	714.473[b,c]
	$4\frac{1}{2}\leftarrow 3\frac{1}{2}$	$+\leftarrow -$	917.613 62(70)	918.084[b]
		$-\leftarrow +$	918.124 59(70)	918.084[b]
	$5\frac{1}{2}\leftarrow 4\frac{1}{2}$	$-\leftarrow +$	1119.283 01(91)	1118.795
		$+\leftarrow -$	1120.401 22(100)	1118.316
3/2	$2\frac{1}{2}\leftarrow 1\frac{1}{2}$	$+\leftarrow -$	537.005 32(51)	536.586[c]
		$-\leftarrow +$	541.291 37(50)	540.524[c]

[a]The figures in parentheses are the 1 standard deviation estimate of the experimental uncertainty, in units of the last quoted decimal place.
[b]Lambda doubling not resolved in the optical spectrum (Ref. 30).
[c]Transition frequency obtained by extrapolation of the optical term values from higher J values.

have been detected by far-infrared LMR spectroscopy. For all but one of these transitions, both lambda-doublet components have been observed. The data have been fitted in a single set by constraining spin-orbit and the base lambda-doubling intervals to values estimated from other sources using the phenomenological model given in Eq. (2). The parameters determined in this fit (the term value, g_J-factor, and two second-order Zeeman parameters for each level involved) are given in Table III.

The zero-field rotational frequencies of FeD obtained from this fit are given in Table V, together with those obtained from the previous optical study of Balfour *et al.*;[30] for optical term values with J less than $3\frac{1}{2}$, it was necessary to extrapolate the mean of the term values and superimpose lambda-doubling intervals using Eqs. (3)–(5). It can be seen that the present measurements provide an improvement by a factor of about 10^3 in accuracy; the optical term values have uncertainties of between 0.02 and 0.03 cm^{-1} (that is, between 0.6 and 0.9 GHz).

In the earlier study of the far-infrared spectrum of FeH by LMR,[10] it proved possible to detect fine-structure transitions between the three lowest spin components as well as the pure rotational transitions. These observations at shorter wavelengths provided accurate measurements of both the fine-structure and the lambda-doubling intervals for FeH. The search for these transitions was greatly aided by a prior knowledge on the fine structure intervals, provided by the analysis of the $F\,^4\Delta$-$X\,^4\Delta$ optical spectrum of FeH (Ref. 8) in which transitions with $\Delta\Omega=\pm 1$ were observed in addition to the dominant $\Delta v=0$ transitions. Unfortunately, such "forbidden" transitions were not identified in the study of the F-X transition of FeD.[30] Some searches for the fine-structure

TABLE VI. Molecular parameters for FeH and FeD in the $v=0$ level of the $X^4\Delta$ state.

Parameter (cm^{-1})	FeH	FeH (Ref. 37)	FeD
A	−98.3603(827)[a]	−116.860(524)	−98.3603
λ	16.1372(619)	10.645(693)	16.1372
η	−0.3573(776)	⋯	−0.3573
γ	−6.0703(399)	⋯	−3.2087
B	6.4997(140)	6.509 07(330)	3.4357[b]
D	$0.193(175)\times 10^{-3}$	$0.23245(833)\times 10^{-3}$	0.849×10^{-4}[b]
λ_D	$0.2781(219)\times 10^{-1}$	⋯	0.147×10^{-1}

[a]The numbers in parentheses are 1 standard deviation in the least-squares fits, in units of the last quoted decimal place.
[b]Value determined by Balfour *et al.* (Ref. 30).

transitions of the FeD radical were made by LMR with laser lines in the 50–60 μm region but no identifiable signals were observed. To aid such work in the future and to provide a connection between the term values for the different spin components in the present work, we have made a best estimate of the fine-structure intervals of FeD from those already known for FeH. The term values determined for FeH by Phillips *et al.*[8] up to $J=8\frac{1}{2}$ (actually the mean of the two lambda doublets) were fitted to the effective Hamiltonian for a molecule in a $^4\Delta$ state;[35] the results are given in Table VI. Three fine structure parameters A, λ, and η are required to model the three different spin-orbit splittings of FeH in its ground state. Using a fairly simple model with seven parameters, it proved possible to fit the term values with a standard deviation of 0.345 cm^{-1}. This figure cannot be regarded as satisfactory since it is about 20 times larger than the experimental uncertainty in the measurement; furthermore, the parameters determined are heavily correlated. The parameter values can be compared with those reported by Dulick *et al.*[37] in a similar fit of the term values (see also Table VI). The large difference in the values determined for the fine structure parameters arises because Dulick *et al.* did not use the $^4\Delta$ effective Hamiltonian to determine them. The fine-structure intervals for FeD were determined from those of FeH by assuming that A, λ, and η are independent of the reduced mass μ, while B, λ, and λ_D are proportional to μ^{-1}. The parameters used for the FeD calculation are also given in Table VI. The values for B and D were taken from the work of Balfour *et al.*,[30] while the values for λ and λ_D were scaled in the ratio of the rotational constants. The resultant fine-structure intervals for FeD are

$$E\left(J=2\tfrac{1}{2},\Omega=5/2,+\right)-E\left(J=3\tfrac{1}{2},\Omega=7/2,-\right)=149.51\ \text{cm}^{-1},$$

$$E\left(J=1\tfrac{1}{2},\Omega=3/2,-\right)-E\left(J=2\tfrac{1}{2},\Omega=5/2,+\right)=199.88\ \text{cm}^{-1}.$$

These values were used to connect the experimental term values for the different spin components, as described in Sec. III C. Since the energy levels of FeH and FeD are obviously perturbed, such estimates of the fine-structure intervals are unlikely to be very reliable, maybe no better than ± 10 cm^{-1}.

The experimental lambda-doubling intervals for the rotational levels studied in this work are given in Table VII. As explained earlier, the first interval for each spin component

TABLE VII. Lambda-doubling intervals for FeD in the $v=0$ level of the $X^4\Delta$ state.

		$\Delta\nu_\Omega$ [a] (MHz)	
Ω	J	Expt.	Calc.[b]
7/2	$3\frac{1}{2}$	1.009	1.009
	$4\frac{1}{2}$	8.01	8.07
	$5\frac{1}{2}$	31.35	36.32
	$6\frac{1}{2}$	94.31	121.08
5/2	$2\frac{1}{2}$	35.77	35.77
	$3\frac{1}{2}$	214.88	214.61
	$4\frac{1}{2}$	725.84	745.76
	$5\frac{1}{2}$	1844.06	2003.01
3/2	$1\frac{1}{2}$	1428.66	1428.66
	$2\frac{1}{2}$	5715.07	5714.64

[a]$\Delta\nu_\Omega$ is defined as $(E_f - E_e)$.
[b]The calculated value is obtained using Eqs. (3), (4), or (5).

was estimated from the formulas given in Eqs. (3)–(5) and constrained to these values in the least-squares fit. The calculated values for the lambda-doubling intervals for the higher J levels are also given in Table VII. The agreement with the experimental values is reasonably good, justifying the use of the procedure. The deviations between the experimental and theoretical numbers increase with J and are explicable as the effects of centrifugal distortion.

The Zeeman parameters determined for FeD are given in Table VIII, together with the corresponding values for FeH.[10] The g_J values for a molecule in a pure $^4\Delta$ state in Hund's case (a) and case (b) limits[36] are also given in Table VIII. It can be seen that the g_J factors for FeD are consistently smaller than those for FeH, reflecting the fact that FeD is closer to Hund's case (a) limit. The second-order Zeeman parameters c_1 and c_2 are expected to be inversely proportional to the rotational constant B. This expectation has been used to estimate the base values for c_1 (for the lowest J value for each spin component), as described in Sec. III C. The ratios of the values for c_1 and c_2 for the FeD and FeH values are also given in Table VIII. The ratios of the c_1 values for the levels with $J \geq \Omega$ are close to the inverse ratio of the B values, justifying the original assumption. However, the ratios for the c_2 values vary widely. It is not clear why this is so but, quite possibly, it reflects local perturbations of the levels.

The present work adds considerably to the accurate database on the FeD (and FeH) radical. Despite this, much further work remains to be done. The additional work on the pure rotational spectrum in the $\Omega=3/2$ and 1/2 spin components required has been mentioned earlier in the paper. There is also a great need to detect fine-structure transitions in FeD since the spin-orbit splittings are not known for this isotopologue. We have attempted to estimate these splittings for the $X\,^4\Delta$ state using the effective Hamiltonian to model them. However, it is known that the ground state levels are strongly perturbed and the model is unlikely to be reliable. In these circumstances, experimental measurement provides the most reliable way to determine them.

ACKNOWLEDGMENTS

The authors are grateful for the support of this work from the National Science Foundation under Grant No. 0802607.

TABLE VIII. Zeeman parameters for FeH and FeD in the $X^4\Delta$ state

			g_J				$10^3 c_1$ (GHz^{-1})			$10^4 c_2$ (GHz^{-1})		
Ω	J	Parity	FeD	FeH	Case (a)	Case (b)	FeD	FeH	Ratio	FeD	FeH	Ratio
7/2	$3\frac{1}{2}$	−	1.202 032	1.248 023	1.1111	1.2381	0.0	0.0000		1.622	0.9899	1.639
		+	1.202 006	1.247 946	1.1111	1.2381	0.0	0.0076		1.641	0.9791	1.676
	$4\frac{1}{2}$	+	0.839 160	0.902 844	0.7071	0.8889	1.9572	0.9841	1.989	−0.0313	0.0984	−0.318
		−	0.839 152	0.902 630	0.7071	0.8889	1.9562	0.9725	2.012	−0.0224	0.1037	−0.216
	$5\frac{1}{2}$	−	0.641 633	0.711 096	0.4895	0.6909	2.5091	1.2537	2.001	−0.1652	−0.0070	23.21
		+	0.641 611	0.710 532	0.4895	0.6909	2.5074	1.2287	2.041	−0.1580	0.0033	−47.88
	$6\frac{1}{2}$	+	0.521 160	0.591 091	0.3590	0.5641	2.6723	1.3205	2.024	−0.1194	−0.0087	13.72
		−	0.521 105	0.590 154	0.3590	0.5641	2.6714	1.2936	2.065	−0.1168	−0.002	58.4
5/2	$2\frac{1}{2}$	+	1.035 865	1.132 507	0.8571	1.1619	0.7681	0.4122	1.863	1.8382	1.336	1.375
		−	1.035 838	1.131 387	0.8571	1.1619	0.7606	0.4082	1.863	1.7695	1.363	1.298
	$3\frac{1}{2}$	−	0.601 066	0.686 094	0.4762	0.7302	2.6796	1.5418	1.738	−0.5057	−0.2212	2.286
		+	0.600 738	0.682 869	0.4762	0.7302	2.6643	1.5007	1.775	−0.5267	−0.1823	2.889
	$4\frac{1}{2}$	+	0.404 190	0.485 076	0.3030	0.5091	3.0240	1.7713	1.707	−0.3944	−0.2041	1.932
		−	0.403 365	0.478 637	0.3030	0.5091	2.9934	1.6416	1.823	−0.3948	−0.1377	2.867
	$5\frac{1}{2}$	+	0.299 069	0.377 72	0.2098	0.3814	3.0892	1.8329	1.695	−0.2450	−0.1361	1.800
		−	0.297 643	0.367 862	0.2098	0.3814	3.0363	1.6129	1.883	−0.2346	−0.0569	4.123
3/2	$1\frac{1}{2}$	−	0.649 106	0.793 974	0.4000	0.9333	2.451	1.262	1.942	1.2349	1.160	1.065
		+	0.642 343	0.772 144	0.4000	0.9333	2.193	1.1295	1.942	1.0966	1.441	0.761
	$2\frac{1}{2}$	+	0.265 852	0.344 630	0.1714	0.3810	3.4640	2.078	1.667	−0.8830	−0.736	1.200
		−	0.254 296	0.311 283	0.1714	0.3810	3.1409	1.8003	1.745	−0.8241	−0.391	2.108

[1] P. K. Carroll and P. McCormack, Astrophys. J. **177**, L33 (1972).
[2] L. Klynning and B. Lindgren, University of Stockholm USIP Report No. 73-20, 1973.
[3] P. K. Carroll, P. McCormack, and S. O'Connor, Astrophys. J. **208**, 903 (1976).
[4] J. D. Kirkpatrick, I. N. Reid, J. Liebert, R. M. Cutri, B. Nelson, C. A. Biechman, C. C. Dahn, D. G. Monet, J. E. Gizis, and M. F. Skrutskie, Astrophys. J. **519**, 802 (1999).
[5] J. D. Kirkpatrick, F. Allard, T. Bida, B. Zuckerman, E. E. Becklin, G. Chabrier, and I. Baraffe, Astrophys. J. **519**, 834 (1999).
[6] J. A. Valenti, C. M. Johns-Krull, and N. P. Piskunov, in *Proceedings of the 11th Cambridge Workshop on Cool Stars, Stellar Systems and the Sun*, edited by R. J. Garcia Lopez, R. Rebolo, and M. R. Zapaterio Osorio [ASP Conf. Ser. 223, 1579 (2001)].
[7] S. R. Langhoff and C. W. Bauschlicher, Jr., J. Mol. Spectrosc. **141**, 243 (1990).
[8] J. G. Phillips, S. P. Davis, B. Lindgren, and W. J. Balfour, Astrophys. J. **65**, (Suppl.), 721 (1987).
[9] C. Wilson, H. M. Cook, and J. M. Brown, J. Chem. Phys. **115**, 5943 (2001).
[10] J. M. Brown, H. Körsgen, S. P. Beaton, and K. M. Evenson, J. Chem. Phys. **124**, 234309 (2006).
[11] P. K. Carroll, P. McCormack, and S. O'Connor, Astron. Astrophys. **26**, 373 (1976).
[12] A. E. Stevens, C. S. Feigerle, and W. C. Lineberger, J. Chem. Phys. **78**, 5420 (1983).
[13] S. P. Beaton, K. M. Evenson, T. Nelis, and J. M. Brown, J. Chem. Phys. **89**, 4446 (1988).
[14] J. P. Towle, J. M. Brown, K. Lipus, E. Bachem, and W. Urban, Mol. Phys. **79**, 835 (1993).
[15] D. A. Fletcher, R. T. Carter, J. M. Brown, and T. C. Steimle, J. Chem. Phys. **93**, 9192 (1990).
[16] R. T. Carter, T. C. Steimle, and J. M. Brown, J. Chem. Phys. **99**, 3166 (1993).
[17] R. T. Carter and J. M. Brown, J. Mol. Spectrosc. **166**, 249 (1994).
[18] R. T. Carter and J. M. Brown, J. Chem. Phys. **101**, 2699 (1994).
[19] D. M. Goodridge, R. T. Carter, J. M. Brown, and T. C. Steimle, J. Chem. Phys. **106**, 4823 (1997).
[20] D. F. Hullah, R. F. Barrow, and J. M. Brown, Mol. Phys. **97**, 93 (1999).
[21] D. M. Goodridge, D. F. Hullah, and J. M. Brown, J. Chem. Phys. **108**, 428 (1998).
[22] D. F. Hullah, C. Wilson, R. F. Barrow, and J. M. Brown, J. Mol. Spectrosc. **192**, 191 (1998).
[23] C. Wilson and J. M. Brown, J. Mol. Spectrosc. **197**, 188 (1999).
[24] C. Wilson and J. M. Brown, Mol. Phys. **99**, 1549 (2001).
[25] W. J. Balfour, J. M. Brown, and L. Wallace, J. Chem. Phys. **121**, 7735 (2004).
[26] C. Wilson and J. M. Brown, J. Mol. Spectrosc. **209**, 192 (2001).
[27] J. M. Brown and A. Carrington, *Rotational Spectroscopy of Diatomic Molecules* (Cambridge University Press, Cambridge, England, 2003).
[28] J. A. Gray, M. Li, and R. W. Field, J. Chem. Phys. **92**, 4651 (1990).
[29] J. A. Gray, M. Li, T. Nelis, and R. W. Field, J. Chem. Phys. **95**, 7164 (1991).
[30] W. J. Balfour, B. Lindgren, and S. O'Connor, Phys. Scr. **28**, 551 (1983).
[31] T. J. Sears, P. R. Bunker, A. R. W. McKellar, K. M. Evenson, D. A. Jennings, and J. M. Brown, J. Chem. Phys. **77**, 5348 (1982).
[32] J. M. Brown and K. M. Evenson, J. Mol. Spectrosc. **98**, 392 (1983).
[33] J. M. Brown and K. M. Evenson, J. Mol. Spectrosc. **136**, 68 (1989).
[34] A. Robinson, J. M. Brown, J. Flores-Mijangos, L. R. Zink, and M. Jackson, Mol. Phys. **105**, 639 (2007).
[35] J. M. Brown, A. S.-C. Cheung, and A. J. Merer, J. Mol. Spectrosc. **124**, 464 (1987).
[36] J. J. Harrison and J. M. Brown, Astrophys. J. **686**, 1426 (2008).
[37] M. Dulick, C. W. Bauschlicher, A. Burrows, C. M. Sharp, R. S. Ram, and P. F. Bernath, Astrophys. J. **594**, 651 (2003).